Attempting to Produce Helium White Dwarfs From Low-Metallicity Solar Mass Stars

Scott Tompkins[1]

[1]*Barrett Honors College at Arizona State University, Tempe, AZ 85287*

Abstract

I examine the effects of metallicity on solar mass stellar evolution, trying to replicate a previous result in *Windhorst et al. (2018)*, in which a zero metallicity solar mass star did not reach the AGB and thus may turn into a helium white dwarf. In trying to replicate this result, I used the *MESA* stellar evolution code and was unable to reproduce this result. While *MESA* has undergone several updates since the previous result was obtained, more current evidence suggests that this may have been a one-time occurrence, as no helium white dwarves were produced for low-metallicity models. Nonetheless, interesting results were obtained, including a lowest metallicity value for which CNO burning does not significantly contribute during the main sequence, 1^{-10} $Z_\odot$, which produces noticeable effects on post main sequence evolution. All models are run with no rotation, one solar mass, and a series of *MESA* parameters kept constant, with the only exception being metallicity.

Keywords: Low-Metallicity, White Dwarfs, AGB, Population III

1. INTRODUCTION

In this paper, using the *MESA* stellar evolution code, I examine the effect of metallicity on the evolution of solar mass stars running metallicity values between 0.02, solar metallicity, and zero metallicity. I attempted to reproduce a result in *Windhorst et al. (2018)* in which a solar mass star of zero metallicity does not reach the AGB, yet a star of 10^{-8} $Z_\odot$ does. I theorized that a limit between 10^{-8} $Z_\odot$ and zero must exist for which the AGB does occur, however, I was unable to replicate the zero metallicity model and even zero metallicity reached the AGB. Limitations in *MESA* meant that I was unable to complete the AGB, but all models did reach shell-helium burning and began to produce C12 in their cores, meaning that had the model been able to progress, the end stage would have been a carbon white dwarf. *MESA* has difficulty with the shell burning phase in which convection develops behind the nuclear burning regions that moves towards the surface while the burning propagates inwards as convectively bounded flames, limited by thermal timescales. As such, timesteps between model updates become lower than one year, meaning that tens or hundreds of thousands of model numbers are required to evolve past this phase with a partially degenerate

satompki@asu.edu

helium core. This phase has always been a problem in *MESA* due to the underlying physics. One can sacrifice accuracy by setting high lower bounds on the time step between models, but for the purposes of this paper, this was not an option as accuracy and physically meaningful models were required.

As such, these results do not support those of *Windhorst et al. (2018)* for which the AGB did not occur at zero metallicity for one solar mass. Despite this, interesting results were obtained, such as the relevance of CNO burning at low metallicity and how this changes the post-main sequence evolution, opacity and structure profiles, and the rate at which a partially degenerate helium core forms. Using the features provided by *MESA* and python, a series of metallicity dependent features are discussed. The first important result found was the change in post-main sequence evolution that abruptly changes between 10^{-10} $Z_\odot$ and 10^{-6} $Z_\odot$. In figure 1, the loop in the 10^{-10} $Z_\odot$ plot occurs when the star has produced enough Carbon-12 in its core to have significant CNO burning, which causes the core to expand, contracting the outer layers while supplying extra energy, which causes a noticeable increase in temperature and luminosity. This does not occur above 10^{-10} $Z_\odot$ because enough C-12 is present to have CNO burning on the main sequence. This demonstrates the importance of CNO cycle burning to solar mass stars, despite it not being a primary source of nuclear energy generation. The feature is indistinguishable for zero, 10^{-14} $Z_\odot$ and 10^{-10} $Z_\odot$, as their overlaid HR diagrams do not show any differences in luminosity or temperature, perhaps indicating that metallicity does not have any significant effect at 1.0 $M_\odot$ until reaching a threshold value of Z.
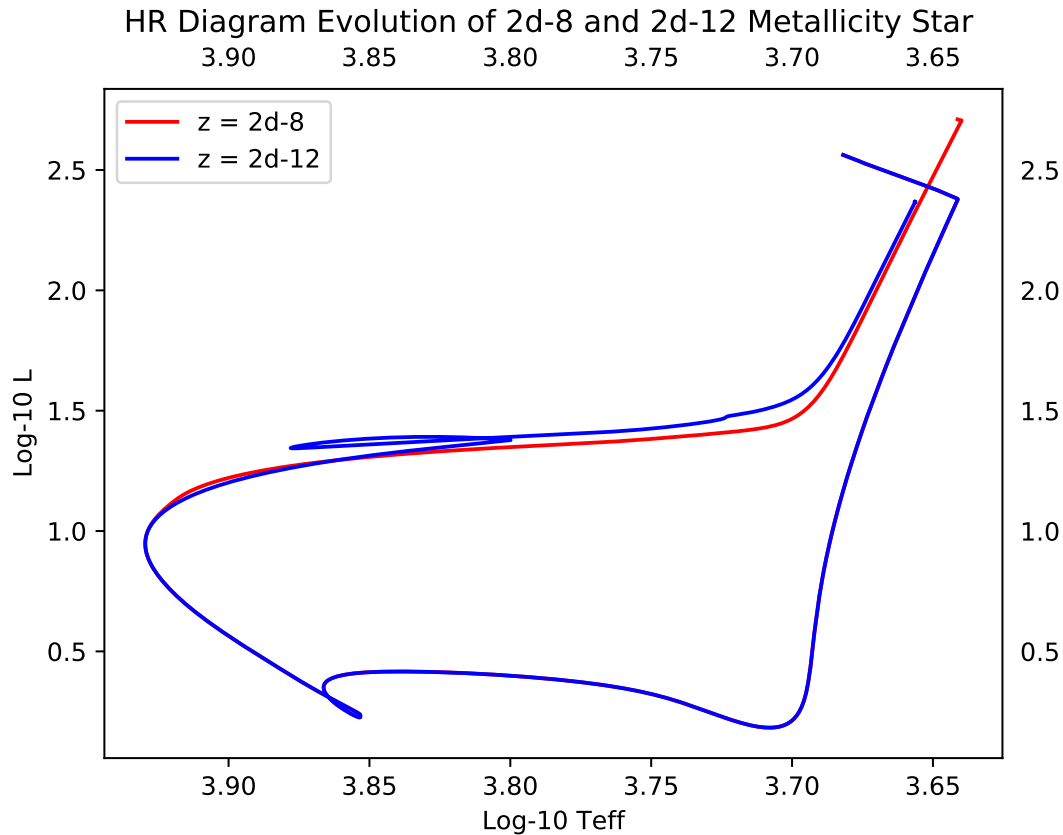
Figure 1. The Hertzsprung-Russel Diagram comparing the evolution 10^{-10} $Z_\odot$ and 10^{-6} $Z_\odot$ solar mass star.

Another result of interest is the rate at which the semi-degenerate helium core forms in the star. While metallicity obviously affects age, the rate at which partially degenerate core forms strongly depends on metallicity. When normalized to one, the core forms over a longer portion of the star's lifetime as metallicity increases. A sample of metallicities for which the difference is obvious are shown in figure 2. This is because as Z increases, CNO cycle burning becomes more important, and because it is heavily localized at the core due to its temperature dependence, this provides a much more efficient way for the star to accumulate helium at it's core, and thus the higher metallicity values produce semi-degenerate helium cores earlier in their evolution, when the age is normalized to one.
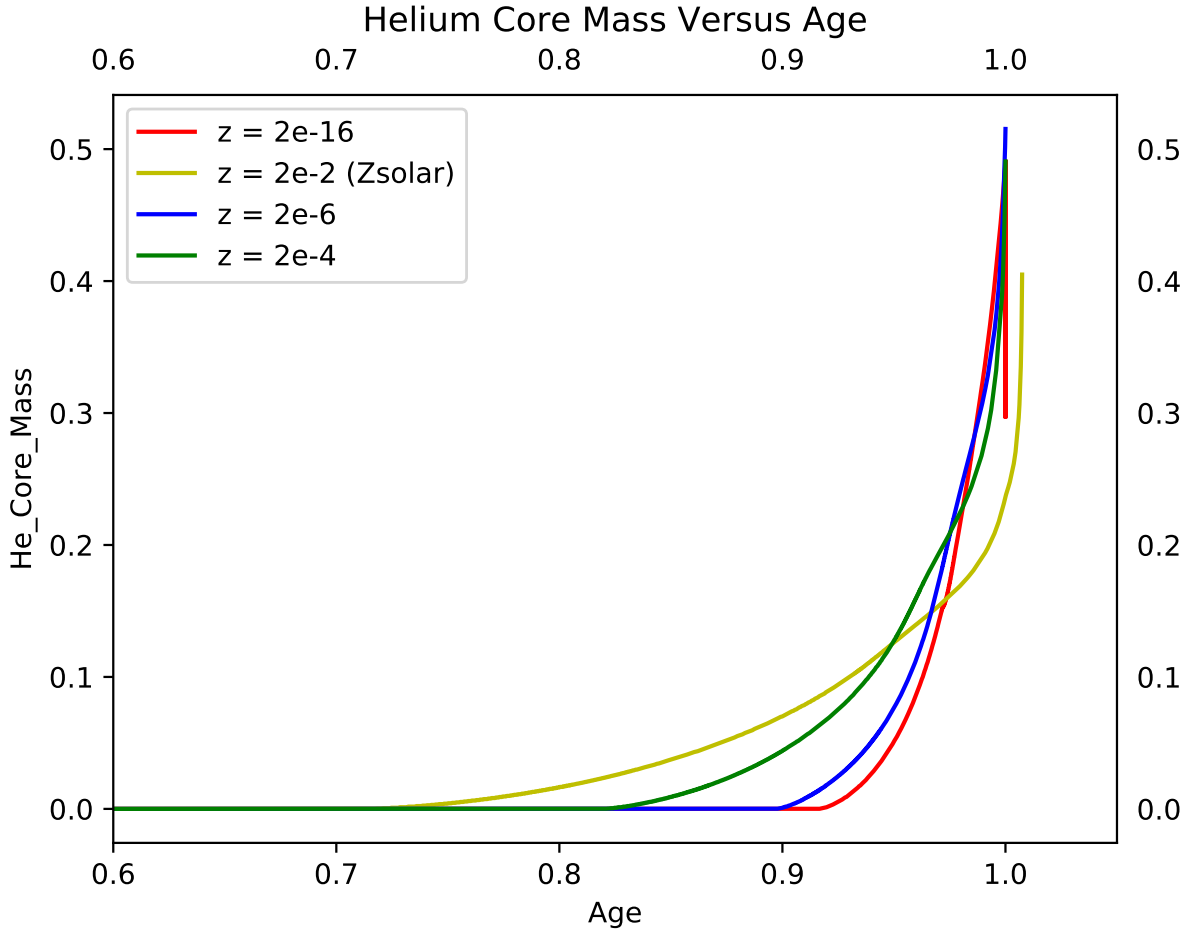
Figure 2. The helium core mass as a function of age *(normalized)* for select metallicities, again, as an absolute mass fraction and not $Z_\odot$. Notice that the the solar mass model, in yellow, begins forming a semi-degenerate core earlier in its evolution than the lower metallicity models, which only form a helium core very late in their evolution.

Metallicity affects stellar evolution primarily through contributing to opacity. Higher metallicity increases the number of free electrons in the core of the star, where all atoms are ionized, leading to free-electron scattering. The major source of opacity lies in the outer layers however, where heavier elements are not completely ionized, and can thus absorb and re-emit light in the outer layers. The opacity caused by heavy elements in the outer layers is significant when comparing the zero and solar metallicity stars at equivalent points in their evolution, when the helium core begins to form, as seen in figure 3. The opacity due to free-electron scattering is visible on the left half of the figure as the solar *(red)* opacity value is higher near the core at high zone numbers. The absorption opacity in the outer layers is visible on the right half of the plot for low zone numbers near the surface, and

shows the significant difference in opacity between zero and solar metallicity models. The opacity is measured as optical depth.
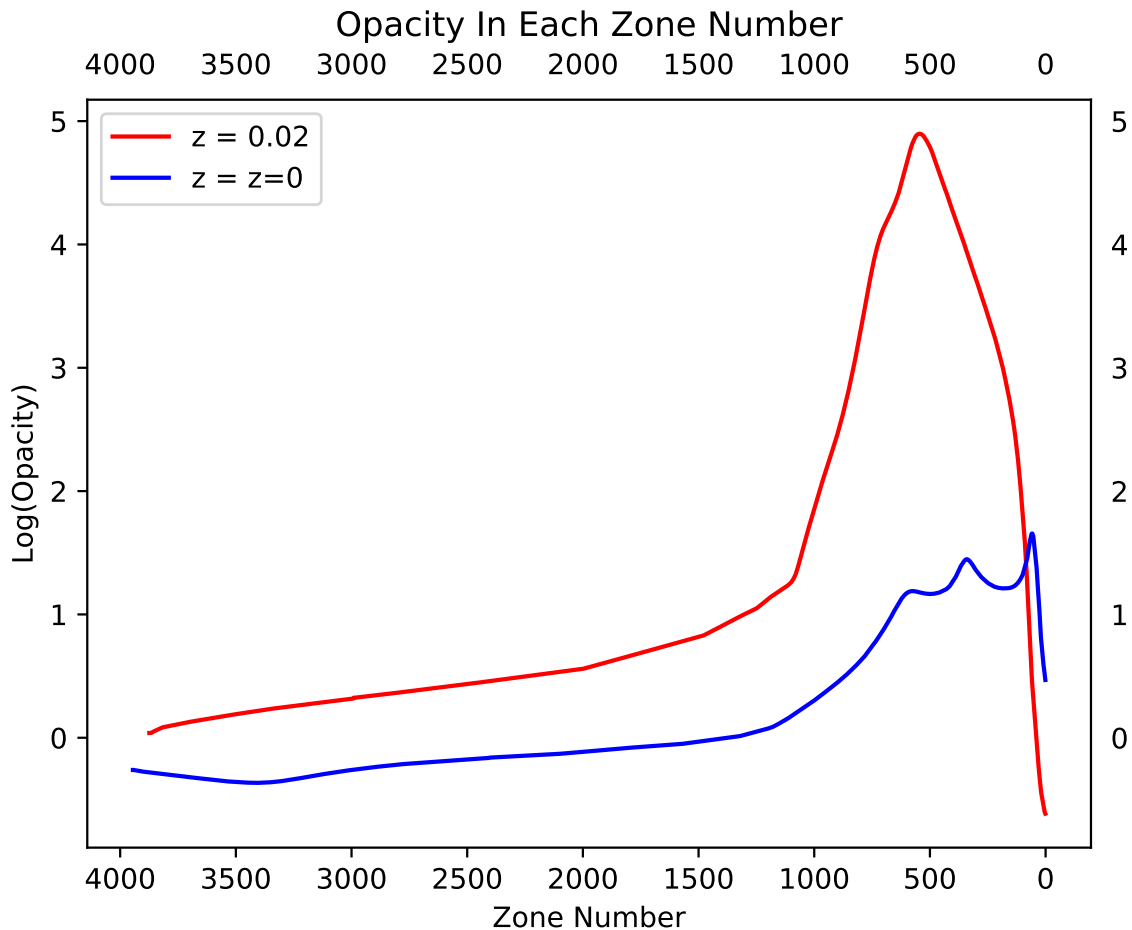
Figure 3. Opacity value in each zone number. The zone numbers are counted from the surface inwards, and thus the x-axis is inverted so that opacity is indirectly plotted versus radius and mass fraction. The zero metallicity model does have a spike in opacity in the same location, but it is a factor of 10^{-5} smaller, and thus it is plotted in a semi-log plot. Note that this opacity profile is taken at an equivalent evolutionary stage, at the onset of helium burning.

2. METALLICITY AND STELLAR EVOLUTION

As discussed in section I, the metallicity significantly affects stellar evolution. With the exception CNO burning beginning during the H-shell burning phase instead of the main sequence at Z values at and above 10^{-6} $Z_\odot$, there appears to be no significant change in the evolution of the solar mass stars until 10^{-4} $Z_\odot$. The 10^{-4} $Z_\odot$ model has a nearly identical main sequence, but high Z values makes it easier for energy generation at the core to support the star, decreasing the rate at which the fuel is burned, which in turn decreases effective temperature and luminosity. While the higher opacity in the outer layers does lead to a larger radius for the star, the change in temperature is more significant in contributing to luminosity.

A noticeably cooler hydrogen shell-burning phase occurs past 10^{-4} $Z_\odot$, and the h-shell burning phase continues to decrease in effective temperature as Z increases. Effective temperature on the main sequence is not significantly affected until a Z value of 10^{-2} $Z_\odot$, or an absolute Z value of 2^{-5}, or a thousandth of $Z_\odot$. After this, each increase in Z causes a significant difference in effective temperature and luminosity. These, however, are well known effects of changing metallicity, and thus do not need further restating. The nontrivial effects of changing Z values are discussed in the following sections.

## 3. EVOLUTIONARY DIFFERENCES BETWEEN ZERO AND SOLAR METALLICITY

In this section I present the HR diagram evolution for each model. They are presented in separate figured as models with similar Z values often do not have significant differences. The entire evolution from the Pre-MS Hayashi track to the termination of each model during the AGB at timestep convergence, which occurs at a point during shell burning on the AGB. The solar and half solar metallicity models converge right at the beginning of helium burning, while all models less than this converge during shell helium burning as the star *MESA* attempts to throw off the outer layers.
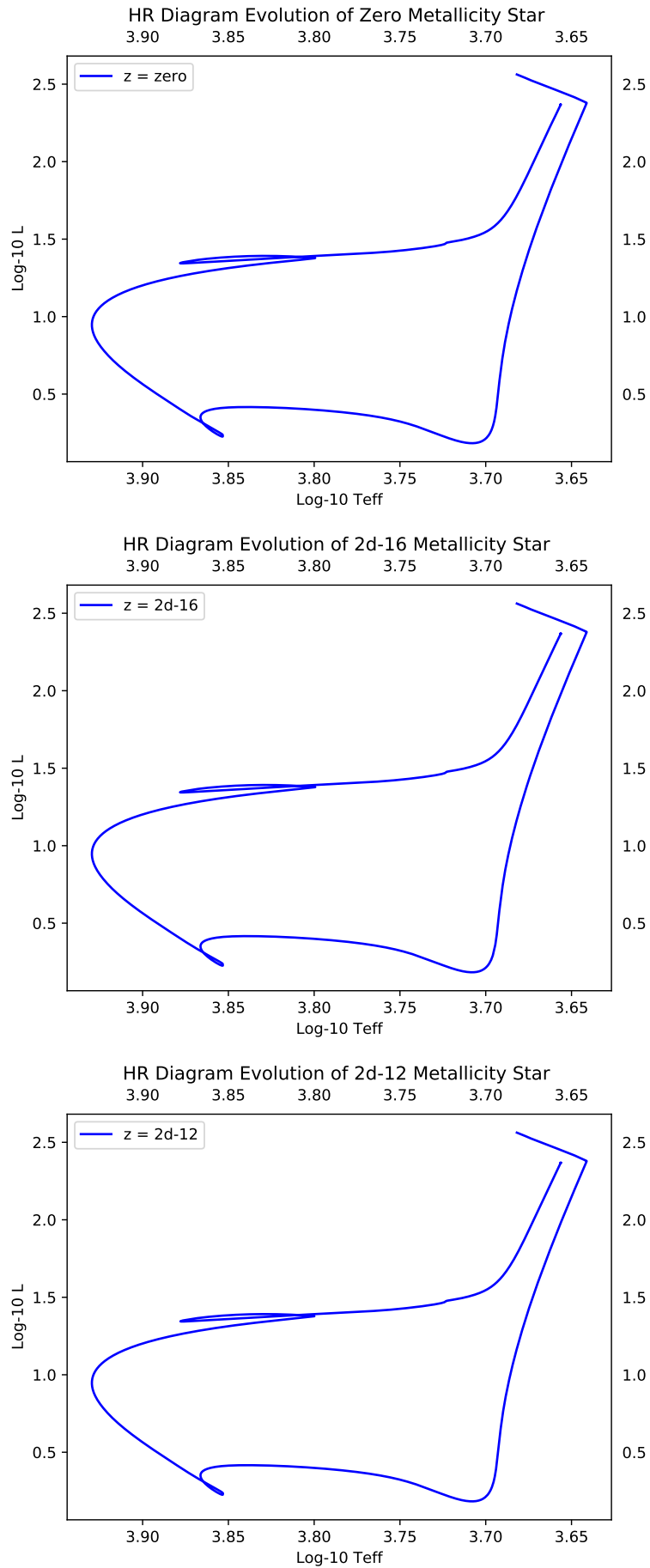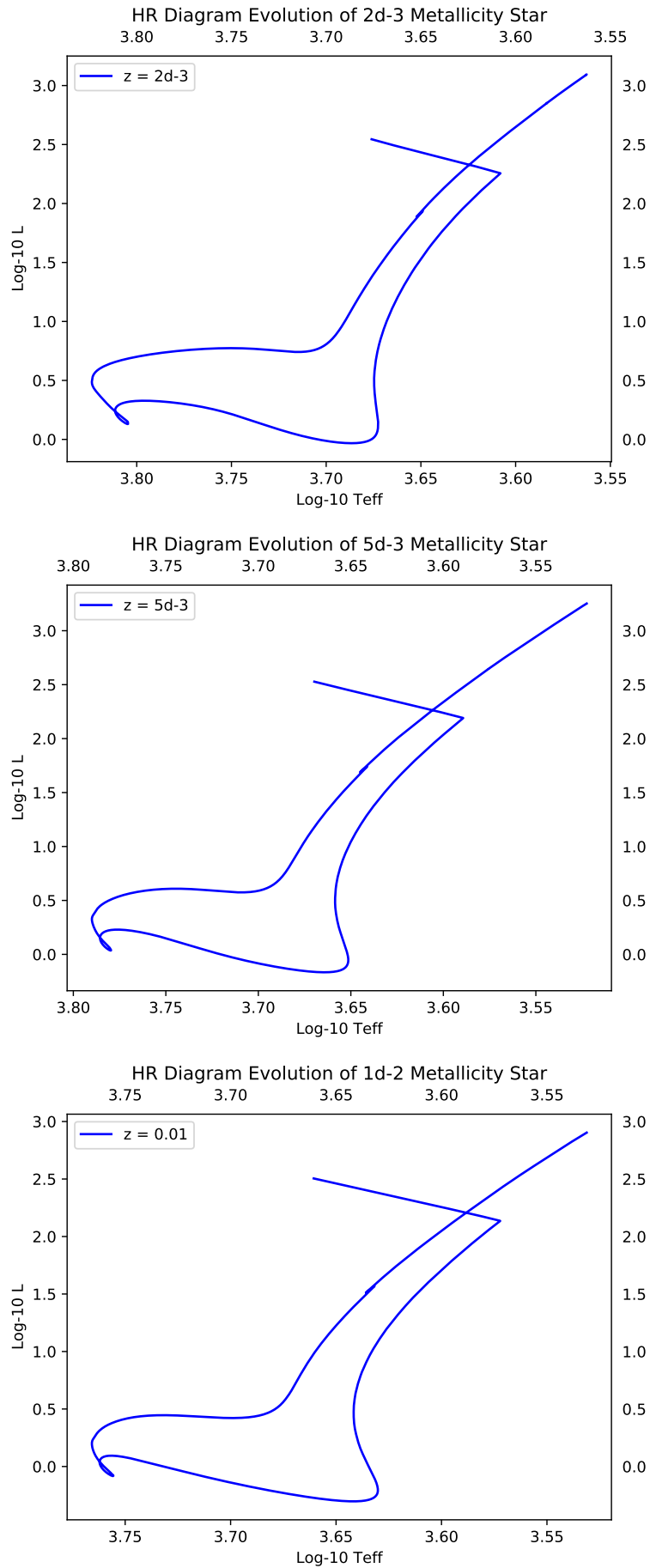
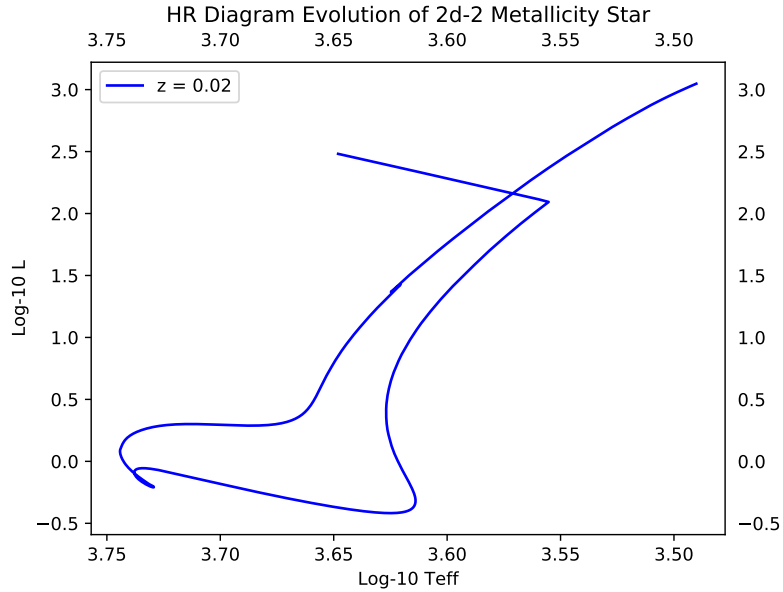**Figure 4.** First set of HR Diagrams, Z=0 to 10^{-10} $Z_\odot$.
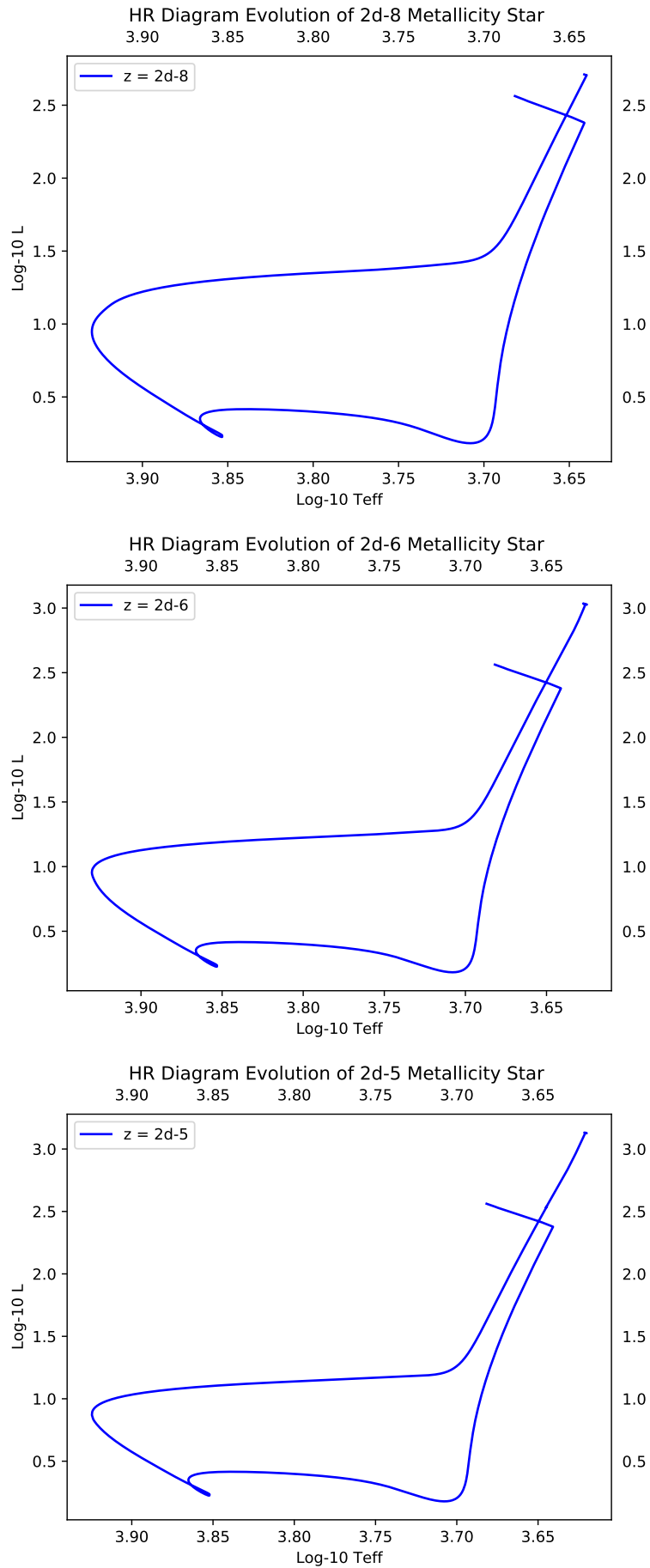
Figure 5. Second set of HR Diagrams, 10^{-6} $Z_\odot$ to 10^{-3} $Z_\odot$.
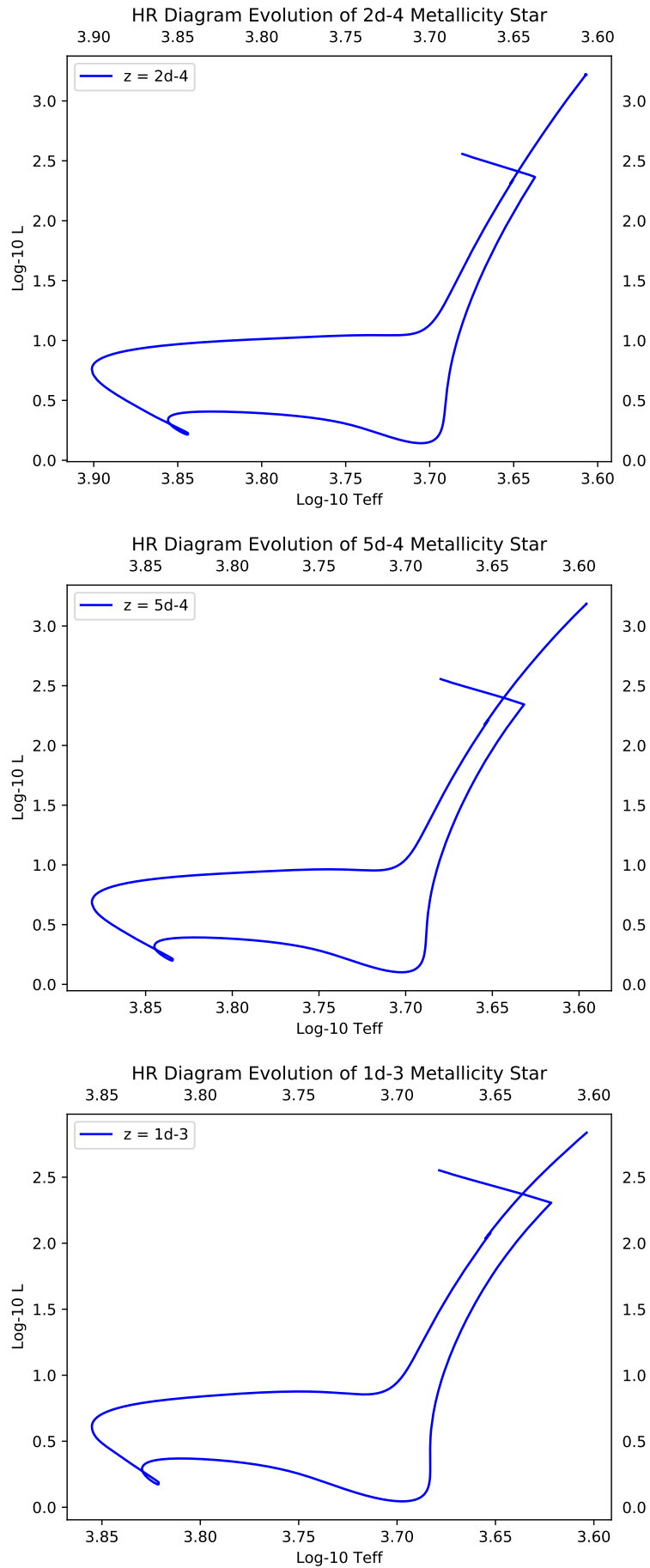
**Figure 6.** Third set of HR Diagrams, $1/100$ $Z_\odot$ to $1/20$ $Z_\odot$.

Figure 7. Fourth Set of HR Diagrams, $1/10$ $Z_{\odot}$ to $1/2$ $Z_{\odot}$.

Figure 8. Final HR Diagram, $Z_\odot$.

### 3.1. *Discussion of Metallicity Dependent Features*

Beyond the obvious features discussed in section II, there are two metallicity dependent features worth discussing. The first and most important feature the absence of CNO burning during the main sequence for values below 10^{-6} $Z_\odot$. This creates structural differences in the stars, which allows burning to take place over a larger mass fraction of the zero metallicity model versus the solar metallicity model. Although CNO burning is not the primary source of energy at 1.0 $M_\odot$, it is still a significant source of energy and thus limits the fraction of the star over which energy generation can occur. The beginning of CNO burning during the H-shell burning phase for the zero, 10^{-14} $Z_\odot$, and 10^{-10} $Z_\odot$ model produces a briefly convective core, something that does not happen in a solar metallicity star. This result is displayed in figures 9 and 10, the Kippenhahn diagrams for zero and solar metallicity, respectively.
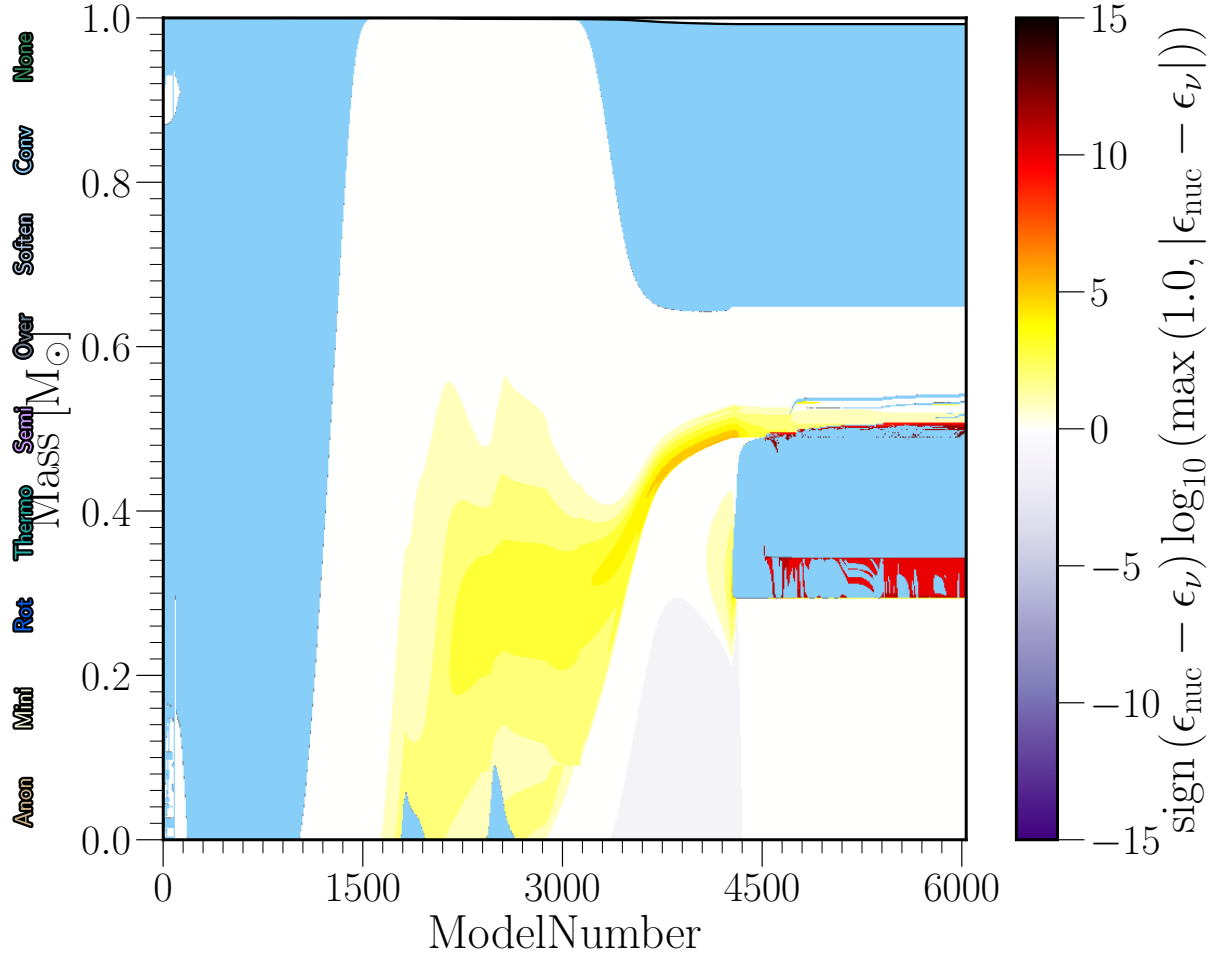
Figure 9. The Kippenhahn diagram for a zero metallicity solar mass star. The core becomes briefly convective between model numbers 2450 and 2600, at the same time when the temperature increase and loop in the HR diagram occurs. Convective regions are represented in blue.

3.2. *Interpreting the Kippenhahn Diagram*

The onset of CNO burning in the core causes brief convection in the core, which is displayed in blue, is present at the beginning of the main sequence for figure 9, the solar mass star. It contributes a low, but not negligible, amount of energy for solar mass and metallicity, which is a feature that persists as Z decreases until the 10^{-10} $Z_\odot$ model, which does have CNO burning during its main sequence, but it is not significant enough to cause any convection in the core until the amount of C12 in the core exceeds a value of around 10^{-12} as a mass fraction. Once reached, this threshold allows CNO burning to contribute significantly to the energy generation. This does not occur above 10^{-10} $Z_\odot$ because the core mass fraction of C12 is above this value and thus CNO cycle burning proceeds gradually over the main sequence, leaving the core radiative, as seen figure 10.
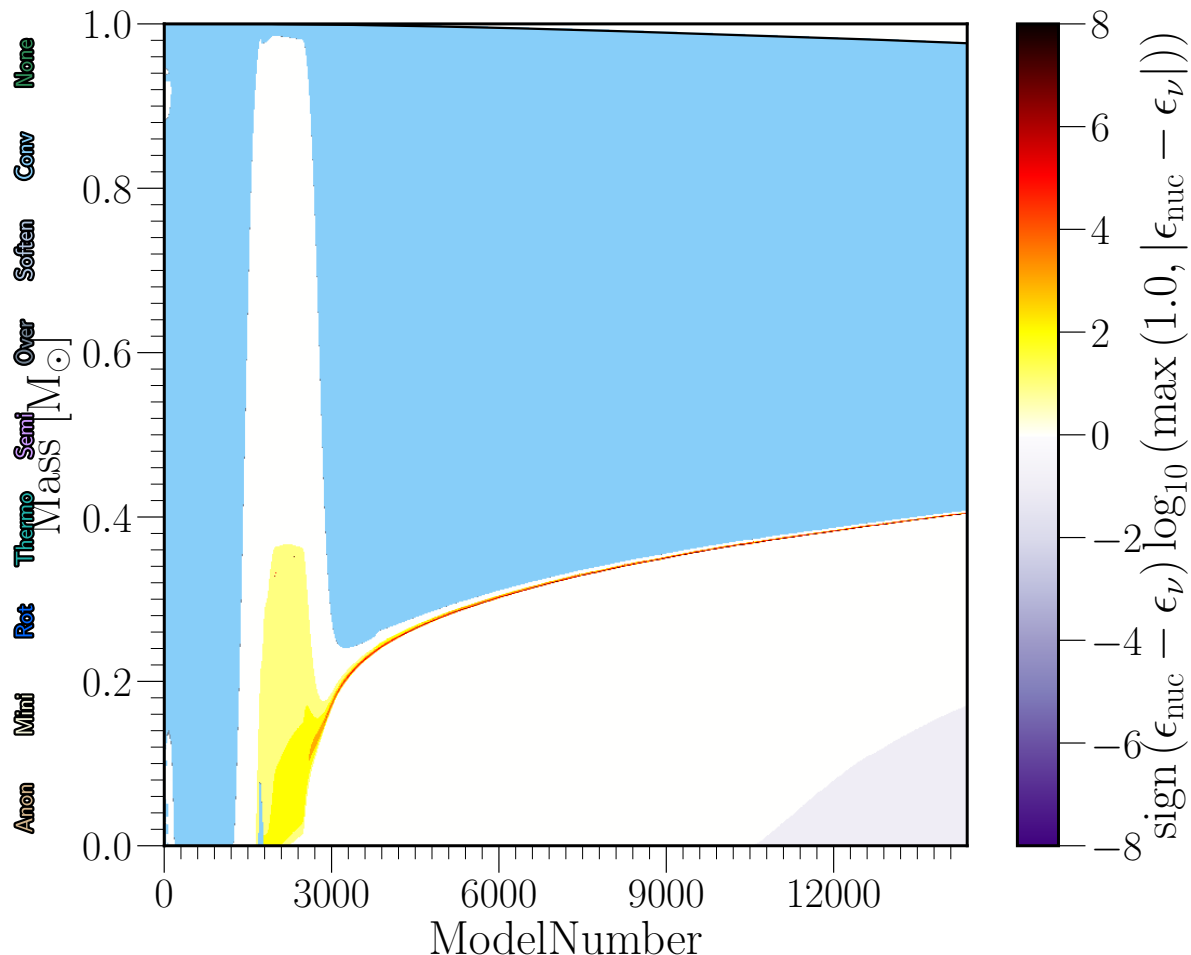
Figure 10. The Kippenhahn diagram for solar metallicity. This model took many more iterations to complete, but the core never becomes convective on or after the main sequence. The core convection in this model occurs as main sequence burning begins, when CNO burning starts, but is only present briefly

4. CONCLUSIONS AND FUTURE WORK

The original objective of this work was to find a low metallicity limit for which a solar mass star does not end as a typical white dwarf, but instead as one made out of helium. This result was initially believed to be possible after a result in *Windhorst et al. (2018)* for zero metallicity ended as a helium white dwarf. This model, however, did not have rotation or mass loss on. Rotation was kept off and the first attempt to replicate the result appeared to be a success, but every model in the first run ended as a helium white dwarf, and the results had to be rejected on physical grounds. Any model with mass loss turned off, also, had to be rejected on physical grounds as well. With the invaluable assistance of Dr. Francis Timmes, a usable set of *MESA* configurations was found, and it produced more realistic results, however, no helium white dwarfs. Even though my original hypothesis about a lowest metallicity value for which a carbon white dwarf would form is refuted by this series of models, interesting discoveries about metallicity and low mass stellar evolution were

made. This investigation highlighted the importance of CNO burning for solar mass stars despite it not being the main source of nuclear energy generation. The lowest three Z values of zero, 10^{-14} $Z_\odot$ and 10^{-10} $Z_\odot$ did not have enough carbon present to begin CNO cycle burning until they began to evolve onto the red giant branch, at which point CNO burning became strong enough for the core to become convective, causing a noticeable increase in effective temperature shown as a loop on the Hertzsprung-Russel diagram.

This phenomena did not occur for higher Z values because the CNO burning was significant enough on the main sequence, and weak enough, to keep the core from becoming convective. In the low metallicity models, CNO burning started over a short timescale, quickly consuming all of the remaining hydrogen in the core before shell burning began. This also helps explain the formation of a semi-degenerate helium core, as CNO burning is a much more localized way for the star to produce helium in the core. A higher mass fraction of He4 at the center allows a helium core to form earlier in the evolution of the star, which is shown in figure 2. Abundance profiles are part of the live feed *MESA* output, and perhaps can be used in future work to study this effect for different masses and/or in more detail.

Finally, the opacity caused by both free-electron scattering in the core, and primarily absorption and re-emission in the outer layers, has a strong dependence on metallicity. The free-electron scattering opacity in the core is visible in figure 3 near the core at high zone number, while absorption produces a much higher opacity in the outer layers with low zone numbers. Opacity is the primary mechanism through which the lower Z models have higher effective temperatures and luminosity, as it becomes much easier for radiation to escape the star with lower metallicity, making the effective temperature higher. This also requires the star to burn nuclear fuel faster, leading to the significant differences in age between high and low Z stars.

Future work will be required to potentially either confirm or refute the result form *Windhorst et al. (2018)* on a solar mass star, but for now evidence shows that a solar mass star will always reach the AGB and ultimately end as a regular carbon white dwarf. While the white dwarf stages was not actually reached for any of the models, helium burning was, indicating that a carbon white dwarf would have been produced. The problem of not completing the AGB can be resolved by either through preventing timestep convergence at the cost of accuracy, or forcing a stronger mass loss through changing the scaling factors. Both of these reduce the accuracy of results, and the first set of discarded runs which produced only helium white dwarves was a result of having a mass loss that was too strong.

5. ACKNOWLEDGMENTS

on the paper itself. Third, the staff and teaching assistants of the 2019 *MESA* Summer School, who taught me to use *MESA* to its fullest potential. Finally, the members of my research group, who provided weekly feedback on the figures and text used in this paper, which proved to be invaluable in its production.

REFERENCES

Hunter, J. D. 2007, Computing In Science & Engineering, 9, 90

Paxton, B., Bildsten, L., Dotter, A., et al. 2011, ApJS, 192, 3

Paxton, B., Cantiello, M., Arras, P., et al. 2013, ApJS, 208, 4

Paxton, B., Marchant, P., Schwab, J., et al. 2015, ApJS, 220, 15

Paxton, B., Bauer, E., Schwab, J., et al. 2018, ApJS, 234, 34

Paxton, B., Smolec, R., Schwab, J., et al. 2019, ApJS, 243, 10

rjfarmer/mesaplot: (Version v1.0.8). https://github.com/rjfarmer/mesaplot/tree/v1.0.8

van der Walt, S., Colbert, S. C., & Varoquaux, G. 2011, Computing in Science Engineering, 13, 22

Windhorst, R. A., Timmes, F. X., Wyithe, J. S. B., et al. 2018, ApJS, 234, 41